https://ntrs.nasa.gov/search.jsp?R=19930085985 2020-06-17T23:32:26+00:00Z

Restriction/Classification Cancelled

FILE COPY
NO

Copy 333
RM L9H29a

NACA RM L9H29a

NACA

RESEARCH MEMORANDUM

INVESTIGATION OF SOME TURBULENT-BOUNDARY-LAYER VELOCITY PROFILES AT A TUNNEL WALL WITH MACH NUMBERS UP TO 1.2

By Marshall P. Tulin and Ray H. Wright

Langley Aeronautical Laboratory
Langley Air Force Base, Va.

THIS DOCUMENT ON LOAN FROM THE FILES OF

NATIONAL ADVISORY COMMITTEE FOR AERONAUTICS
LANGLEY AERONAUTICAL LABORATORY
LANGLEY FIELD, HAMPTON, VIRGINIA

RETURN TO THE ABOVE ADDRESS.

REQUESTS FOR PUBLICATIONS SHOULD BE ADDRESSED AS FOLLOWS:

NATIONAL ADVISORY COMMITTEE FOR AERONAUTICS
1512 H STREET, N. W.
WASHINGTON 25, D. C.

CLASSIFICATION CHANGED TO
UNCLASSIFIED DATE 8-18-54
AUTHORITY J.W. CROWLEY
CHANGE #2461 F.E.T.

Restriction/ Classification Cancelled

This ... tion ... affect... ited ... State... Act, ... USC ... the ... revel... an ... unaut... law. ... Infor... ited ... only ... ival ... servi... late ... civili... ral ... Gover... rest ... there... own ... loyalty and discretion who of necessity must be informed thereof.

NATIONAL ADVISORY COMMITTEE FOR AERONAUTICS

WASHINGTON
November 9, 1949

Restriction/Classification Cancelled

Restriction/Classification Cancelled

NATIONAL ADVISORY COMMITTEE FOR AERONAUTICS

RESEARCH MEMORANDUM

INVESTIGATION OF SOME TURBULENT-BOUNDARY-LAYER VELOCITY PROFILES AT A TUNNEL WALL WITH MACH NUMBERS UP TO 1.2

By Marshall P. Tulin and Ray H. Wright

SUMMARY

Turbulent-boundary-layer profiles at large Reynolds numbers and with Mach numbers up to 1.2 are presented. Under the conditions of this investigation, the velocity profile shapes were substantially unaffected by compressibility. The nondimensional profile shape was found to be a function only of the parameter H_i $\left(H_i = \frac{\delta_i}{\theta_i}\right.$, where δ_i and θ_i are the displacement thickness and momentum thickness, respectively, which would be obtained if the velocity profiles were analyzed as for the incompressible flow$\left.\right)$. At a Mach number of 1.2 and with the low values of H_i existing for this investigation, the turbulent boundary layer under the shock did not separate. The increase in displacement thickness across the shock could be calculated by use of the momentum equation.

INTRODUCTION

An investigation of turbulent-boundary-layer profiles at large Reynolds numbers and Mach numbers up to 1.2 was carried out in connection with the design and investigation of a circular supersonic nozzle for Mach number 1.2. No systematic variation of the variables influencing the boundary-layer development was attempted. Only the boundary-layer profiles existing at various positions on the nozzle wall were investigated.

The results obtained in this investigation are turbulent-boundary-layer-profile data at large Reynolds numbers, of the order of 40,000 based on the momentum thickness, and at Mach numbers up to 1.2. The effects of compressibility on the velocity profile shapes and form parameters were investigated. Some boundary-layer shock-interaction data are presented.

The experimental data obtained are of considerable value, particularly because no experimental work investigating the effect of compressibility on the turbulent-velocity profile shapes has previously been

Restriction/Classification Cancelled

reported, although semiempirical methods for calculating the thickness of the incompressible turbulent boundary layer have, by the use of reasonable assumptions, been extended to compressible flow (reference 1).

SYMBOLS

H_c ratio of displacement thickness to momentum thickness for compressible flow $\left(\frac{\delta_c^*}{\theta_c}\right)$

H_i ratio of displacement thickness to momentum thickness for incompressible flow $\left(\frac{\delta_i^*}{\theta_i}\right)$

M Mach number outside boundary layer

R_{θ_c} Reynolds number based on boundary-layer momentum thickness $\left(\frac{\rho_\delta U \theta_c}{\mu_\delta}\right)$

T_o absolute stagnation temperature inside boundary layer

T_{o_δ} absolute stagnation temperature at outer edge of boundary layer

u velocity inside boundary layer

U velocity outside boundary layer

x distance from throat, positive downstream

y distance normal to surface

δ distance from surface to outer limit of boundary layer

δ_c^* boundary-layer displacement thickness for compressible flow $\left(\int_0^\delta \left(1 - \frac{\rho u}{\rho_\delta U}\right) dy\right)$

δ_i^* boundary-layer displacement thickness for incompressible flow $\left(\int_0^\delta \left(1 - \frac{u}{U}\right)dy\right)$

θ_c boundary-layer momentum thickness for compressible flow $\left(\int_0^\delta \frac{\rho u}{\rho_\delta U}\left(1 - \frac{u}{U}\right)dy\right)$

θ_i boundary-layer momentum thickness for incompressible flow $\left(\int_0^\delta \frac{u}{U}\left(1 - \frac{u}{U}\right)dy\right)$

μ_δ coefficient of viscosity at outer edge of boundary layer

ρ density inside boundary layer

ρ_δ density at outer edge of boundary layer

APPARATUS AND METHODS

This investigation was carried out in the Langley 8-foot high-speed tunnel. The Reynolds number per foot was of the order of 3×10^6 and varied from 18,000 to 64,000 based on the boundary-layer momentum thickness. The variation in Mach number was continuous up to nearly 1.00, but only one supersonic Mach number, approximately 1.2, was attainable with approximately zero pressure gradient at the measuring station. Mach numbers between 1.00 and 1.2 existed only in the accelerating flow between the throat and the supersonic test section. Except for the possibility of moving to various positions along the nozzle, the boundary-layer Reynolds number was not varied independently of the Mach number, and only two regions existed, one near the throat and the other at the supersonic test section, where the pressure gradients were approximately zero.

The principal measuring stations are indicated in figure 1, which also shows the nozzle profile shape along with representative Mach number distributions. The data presented in figures 2 and 3(a) were obtained at these stations. In these figures identification of the test conditions is facilitated by the values of x and M given. It will be noted that for the data of figures 2 and 3(a) long regions of

accelerating flow preceded the test positions. For the general analysis of figure 4, data from various positions on the wall of the nozzle and also from a previously used subsonic test section are included. The data presented in figures 5 and 6 were obtained under the normal shock terminating the supersonic flow at the downstream end of the supersonic test section (see fig. 1).

In order to find out whether the boundary-layer development was affected by condensation of water vapor, measurements were taken with the tunnel sufficiently cool to cause considerable fog in the flow, and these measurements were compared with those taken at much higher temperatures. No appreciable difference appeared in the boundary-layer measurements.

The methods of reference 1, in combination with some boundary-layer measurements in the entrance cone of the tunnel, were employed in computing the boundary-layer displacement thickness used in the design of the supersonic nozzle. The success of the nozzle designed in producing the design supersonic flow attested to the over-all accuracy of the boundary-layer calculations; but because of local pressure gradients at the walls and because of asymmetry angularly about the tunnel wall of the wall boundary layer (the cause of this asymmetry has not been determined) the boundary-layer calculations could not be accurately checked by means of boundary-layer surveys along a single axial line. The present paper is therefore limited to the investigation of boundary-layer profiles and of the behavior of the turbulent boundary layer under the terminal normal shock.

The total pressures through the boundary layer were measured by means of banks of tubes open to the oncoming flow. The banks were of two sizes extending outward into the flow 3 inches and 6 inches, respectively. For the first 3 inches the total-pressure tubes were spaced at $\frac{1}{4}$-inch intervals measured from center to center. On the 6-inch banks the tubes were spaced at $\frac{1}{2}$-inch intervals, measured from center to center, over the outer 3 inches. The pressure differences were measured and photographically recorded on manometers containing tetrabromoethane. Only data near a Mach number of 0.5 and above are presented. The total-pressure tubes used were of 0.050-inch-outside-diameter tubing. In a few cases the total-pressure tubes were interspersed with total (stagnation) temperature probes constructed by placing small thermocouple heads at the entrances to total-pressure tubes; 0.060-inch-outside-diameter tubing was used for these probes. Temperature probes calibrated in the free stream where the stagnation temperature is known showed only small corrections required. With the small supersonic Mach numbers encountered in this investigation, the corrections to the total pressure were small.

For taking accurate measurements of the boundary-layer profile at a given point over a period of time, single total-pressure, static-pressure, and temperature probes were mounted on a micrometer screw. With this apparatus the position of the tubes was continuously variable from the wall outward to 3 inches from the wall.

For most of the surveys the static pressure was obtained from measurements of the pressure at orifices in the tunnel wall. These orifices were 0.031 inch in diameter. Except in the region under the terminal normal shock, the pressure gradients were sufficiently small to cause the static pressure to be essentially constant through the boundary layer.

Mach numbers were obtained from the ratio of static pressure to total pressure. Velocity and density were computed under the assumption of constant stagnation temperature through the boundary layer. Under operating conditions the stagnation temperature in the tunnel normally rises as much as 140° F, but because of inadequate mixing of the cooling air, the temperature near the wall was as much as 50° less than that near the center of the tunnel.

The boundary-layer data have been reduced as if they had been obtained on a flat rather than a cylindrical surface. Because the 4-foot radius is sufficiently large, the error due to this simplication in calculation of the momentum thickness θ_c and of the displacement thickness δ_c^* is less than 2 percent and that in the form parameter $H_c = \frac{\delta_c^*}{\theta_c}$ is negligible.

RESULTS AND DISCUSSION

Temperature considerations.— Temperature data obtained were incomplete and not sufficiently reliable to permit the exact calculation of velocities within the boundary layer and of the boundary-layer displacement and momentum thicknesses. The values of these quantities presented herein are therefore based on the assumption that the stagnation temperature is constant throughout the boundary layer. Some stagnation-temperature profiles, which, however, are not regarded as completely reliable because each profile was taken point by point over a period of time during which steady temperature conditions may not have existed, indicated a maximum change in absolute stagnation temperature throughout the boundary layer not exceeding ±6 percent. At a Mach number of 1.2, the largest for these tests, the absolute stagnation

temperature exceeds the stream temperature by somewhat less than 30 percent of the stream temperature; and if, as has been found by other investigations, with a turbulent boundary layer approximately 90 percent of this temperature difference is recovered at the wall provided no heat transfer takes place through the wall, the change in stagnation temperature through the boundary layer at this Mach number is about 3 percent. With these considerations in mind, a linear variation of stagnation temperature amounting to a 6-percent decrease at the wall was assumed, and the resulting errors involved in assuming constant stagnation temperature were estimated. The following percentage errors were found in the various quantities:

Quantity	Maximum error (percent)
u	3
δ_i	−9
θ_i	−7
H_i	−2
δ_c	7
θ_c	−10
H_c	19

The probable errors are, of course, much less than these maximum values. In particular the values of u and H_i presented herein are not believed to be appreciably in error on account of the stagnation-temperature variation.

Velocity profiles.- Typical velocity profiles with Mach numbers from 0.5 to 1.19 are shown in figure 2. The velocity within the boundary layer u in terms of the velocity U outside the boundary layer is plotted against the nondimensional distance normal to the wall y/θ_i, where θ_i is the value of the boundary-layer momentum thickness that would be obtained from a plot of u/U against y if the flow were assumed incompressible.

With incompressible flows, all nondimensional turbulent-boundary-layer profile shapes have been found to be approximately functions of the single parameter

$$H_i = \frac{\delta_i^*}{\theta_i} \tag{1}$$

(See, for instance, reference 2.) It is of interest to discover whether a similar relation holds also with compressible flow. The compressible nondimensional velocity profiles have therefore been analyzed as if they applied to incompressible flow. The values of δ_i^*, θ_i, and their ratio H_i have been determined, and values of u/U at various values of y/θ_i have been plotted against H_i in figure 4. The symbols apply to the data of this investigation, which include measurements at Mach numbers from 0.5 to 1.2 with variations in Reynolds number caused by changes in speed and variations in position along the tunnel wall. In some cases, the pressure gradients immediately upstream from the measuring position are positive and in some cases negative. Measurements in the boundary layer under normal shock are also included. The solid lines in figure 4 are taken from the low-speed data of reference 2. Since all the u/U values at each value of y/θ_i arrange themselves approximately into single lines, that is, a definite value of u/U corresponds to each value of y/θ_i for each H_i value, it may be concluded that the nondimensional velocity profile shape in compressible, as well as in incompressible flow, is approximately a function of the single parameter H_i. Furthermore, because the data of this paper agree approximately with the low-speed data of reference 2 (note approximate agreement between lines and symbols in fig. 4), the functional relation between H_i and the profile shape is the same for compressible as for incompressible flow, and thus could be approximately represented by a formula of the type $\frac{u}{U} = \left(\frac{y}{\delta}\right)^{1/m}$ as in reference 1.

Most of the values of H_i found in this investigation are smaller than those reported in reference 2. (See fig. 4.) The reason for the small values of H_i obtained is believed to be the existence of the long region of accelerating flow which, in most cases, preceded the measuring point. The large Reynolds number R_θ is also favorable to low values of H_i. Values of H_i as great as 1.3 were obtained only in the region of shock.

Because the profile shapes depend on H_i, the effects of compressibility on the profile shapes can be examined by investigating the variation of that parameter with Mach number. No exact study of the variation of H_i with Mach number can be made from the data of this investigation, because the conditions of the tests could not be so controlled as to maintain constant other variables, such as pressure gradient and boundary-layer Reynolds number, on which the development of H_i might depend. The principal survey stations (fig. 1) were specially chosen,

however, to minimize these extraneous effects, and values of H_i obtained from velocity profiles at these stations have been plotted against Mach number in figure 3(a). The values of H_i for Mach numbers less than 0.9 were obtained at a single station and, in all cases, similar flow conditions prevailed. The pressure gradients at the survey stations were nearly zero and each of the three survey stations was preceded by a long region of accelerating flow (see fig. 1). The survey station for a Mach number of 1.19 was a considerable distance downstream of the other two stations and was, therefore, preceded by additional accelerating flow. This condition may account for the fact that the H_i value at that station is somewhat less than the values found at the upstream positions. With incompressible flow and with the pressure-gradient conditions existing for these data, such relatively small values of H_i change very slowly and it is therefore reasonable to suppose that in the present case these conditions exert only a minor influence. It seems unlikely in any case that H_i variations due to other causes could approximately compensate any variations due to changes in Mach number. The approximate constancy of the H_i values in figure 3(a) is therefore taken as an indication that H_i and hence also the nondimensional velocity profile shape are not greatly affected by compressibility; that is, for the conditions of the present investigation the profile shapes are essentially unaffected by compressibility.

Important because of its occurrence in the momentum equation used in the boundary-layer calculations is the quantity

$$H_c = \frac{\delta_c^*}{\theta_c} \tag{2}$$

where δ_c^* is the actual boundary-layer displacement thickness and θ_c is the actual momentum thickness:

$$\delta_c^* = \theta_i \int_0^{\delta/\theta_i} \left(1 - \frac{\rho u}{\rho_\delta U}\right) d\frac{y}{\theta_i} \tag{3}$$

$$\theta_c = \theta_i \int_0^{\delta/\theta_i} \frac{\rho u}{\rho_\delta U}\left(1 - \frac{u}{U}\right) d\frac{y}{\theta_i} \tag{4}$$

Because in these equations the velocity ratios u/U at fixed values of y/θ_i are unaffected by compressibility, H_c must be dependent on the density ratios ρ/ρ_δ. In the absence of a pressure gradient through the boundary layer, the density depends only on the temperature, which,

with an insulated boundary, increases from stream temperature outside the boundary layer to a value almost equal to stream stagnation temperature at the wall. Because the difference between stagnation temperature and stream temperature increases with Mach number, the density ratio and thereby also H_c depend on the Mach number. This dependence is shown in figure 3(b) where, for a velocity profile

$$\frac{u}{U} = \left(\frac{y}{\delta}\right)^{1/8}$$

that yields a value of H_i equal to about 1.25, H_c is shown plotted against Mach number. For the top curve (fig. 3(b)) the stagnation temperature is assumed constant.

In order to show the sensitivity of H_c to the temperature distribution through the boundary layer, values of H_c have been computed for two cases of cooling at the wall. In both cases, a temperature at the wall 6 percent less than the absolute stagnation temperature of the stream has been assumed. Stagnation-temperature distributions through the boundary layer have been chosen similar to velocity profiles

$$\frac{T_o}{T_{o_\delta}} = 0.94 + 0.06\left(\frac{y}{\delta}\right)^{1/n}$$

Variations of H_c for $n = 5$ and $n = 8$ are shown (fig. 3(b)). The cooling has a substantial effect on the values of H_c, though less than if the linear temperature distribution used for estimating the possible errors due to neglecting the stagnation-temperature variation had been assumed.

From equations (3) and (4) it is evident, because the density within the boundary layer is decreased on account of the temperature increase, that with a given velocity profile $\left(\frac{u}{U} \text{ against } y\right)$ the displacement thickness δ_c^* is increased and the momentum thickness θ_c is decreased by compressibility. With a constant value of θ_c, which is the usual condition for flat-plate flow (see discussion and references of reference 1 concerning absence of compressibility effect on skin friction), the displacement thickness must increase still more with increase in Mach number. Thus, the usual effect of compressibility on the turbulent boundary layer is to increase its displacement.

Turbulent boundary layer under normal shock.- Figure 5 shows the variation of indicated (from wall pressures) Mach number M, displacement thickness δ_c^*, and form parameter H_i through the region under a normal shock near the end of the supersonic test section. In order to facilitate the experiment, the shock wave was moved past the bank of survey tubes rather than vice versa. This process renders the Mach number inaccurate, because for downstream points in figure 5 the Mach number preceding the shock is actually lower than that shown. Nevertheless the phenomena shown are believed to be qualitatively correct, and the experimental method used has the advantage that the effects shown occur at a given station and variations due to movement from one position to another in the tunnel are eliminated. Because the only changes involved are changes in Mach number distribution, the variations shown are due solely to primary or secondary effects of changes in Mach number and Mach number gradient. Because of the very thick boundary layer ($\delta_c^* \approx 0.5$ inch) and, also perhaps, partly because of the observed unsteadiness in shock position, the region of large pressure gradient at the wall is spread over a distance of some 15 inches.

The sharp increase in displacement thickness with decrease in velocity as the shock is moved upstream past the survey position should be noted (fig. 5). This thickening is, of course, to be expected. By assuming that the inertia terms were predominant for the flow through the shock and by choosing from figure 6 a value of H_c, which in this case was constant through the shock, the momentum equation could be used for computing the boundary-layer displacement thickness. True, some of the approximations involved in that equation, particularly as to constancy of pressure through the boundary layer and thinness of the region of pressure jump under the shock, are not well satisfied. Nevertheless, a point so computed (approximate theory in fig. 5) falls near the experimental curve. It seems quite likely, therefore, that with Reynolds numbers sufficiently large to insure turbulent boundary layers the approximate theory may serve as a useful guide to the behavior of the boundary layer under shock.

As may be observed from figure 5, the quantity H_i, which characterizes the shape of the velocity profiles, undergoes the expected increase in the region of positive pressure gradient under shock. The variation in the parameter H_c accompanying this increase in H_i through the shock should not be expected to be as great because of the effect of the decreasing Mach number in reducing H_c. The exact behavior of H_c is dependent on the stagnation-temperature profile. Figure 6 shows the variation of values of H_c calculated on the basis of a constant stagnation temperature throughout the boundary layer. From this condition, H_c is observed to be nearly constant throughout the region of shock.

Because of the relatively small values of the supersonic Mach number attained, the variations of the boundary-layer characteristics in the region under the normal shock were less than those reported in reference 3, for which Mach numbers up to 1.4 existed. In the present investigation no evidence of separation was found, though special efforts were made to detect it. With higher Mach numbers and, consequently, more severe shocks, separation is to be expected at least locally.

CONCLUSIONS

From the results of an investigation of turbulent-boundary-layer profiles at large Reynolds numbers and with Mach numbers up to 1.2, the following conclusions are made:

1. At low values of the velocity-profile-shape parameter H_i $\left(H_i = \frac{\delta_i}{\theta_i} \right.$, where δ_i and θ_i are the displacement thickness and momentum thickness, respectively, which would be obtained if the velocity profiles were analyzed as for incompressible flow$\left.\right)$ found in this investigation, no important effects of compressibility on turbulent-boundary-layer profile shapes at large values of Reynolds numbers were found.

2. With compressible flow, as with incompressible flow, the profile shape is a function of the single parameter H_i.

3. With a given value of H_i the ratio H_c of actual displacement thickness to actual momentum thickness is a function of Mach number and of the stagnation-temperature distribution through the boundary layer.

4. Because of the heating within the boundary layer, its displacement thickness is increased with increase in Mach number.

5. The pressure jump through the shock is spread over a distance at the surface that is large compared with the boundary-layer displacement thickness.

6. With the comparatively weak normal shock corresponding to a Mach number of 1.2 and with a comparatively low value of H_i upstream of the shock, separation of the turbulent boundary layer did not occur.

7. For the conditions of this investigation, the momentum equation could be used for calculating the increase in displacement thickness across the shock.

Langley Aeronautical Laboratory
National Advisory Committee for Aeronautics
Langley Air Force Base, Va.

REFERENCES

1. Tetervin, Neal: Approximate Formulas for the Computation of Turbulent Boundary-Layer Momentum Thicknesses in Compressible Flows. NACA ACR L6A22, 1946.

2. Von Doenhoff, Albert E., and Tetervin, Neal: Determination of General Relations for the Behavior of Turbulent Boundary Layers. NACA Rep. 772, 1943.

3. Zalovcik, John A., and Luke, Ernest P.: Some Flight Measurements of Pressure-Distribution and Boundary-Layer Characteristics in the Presence of Shock. NACA RM L8C22, 1948.

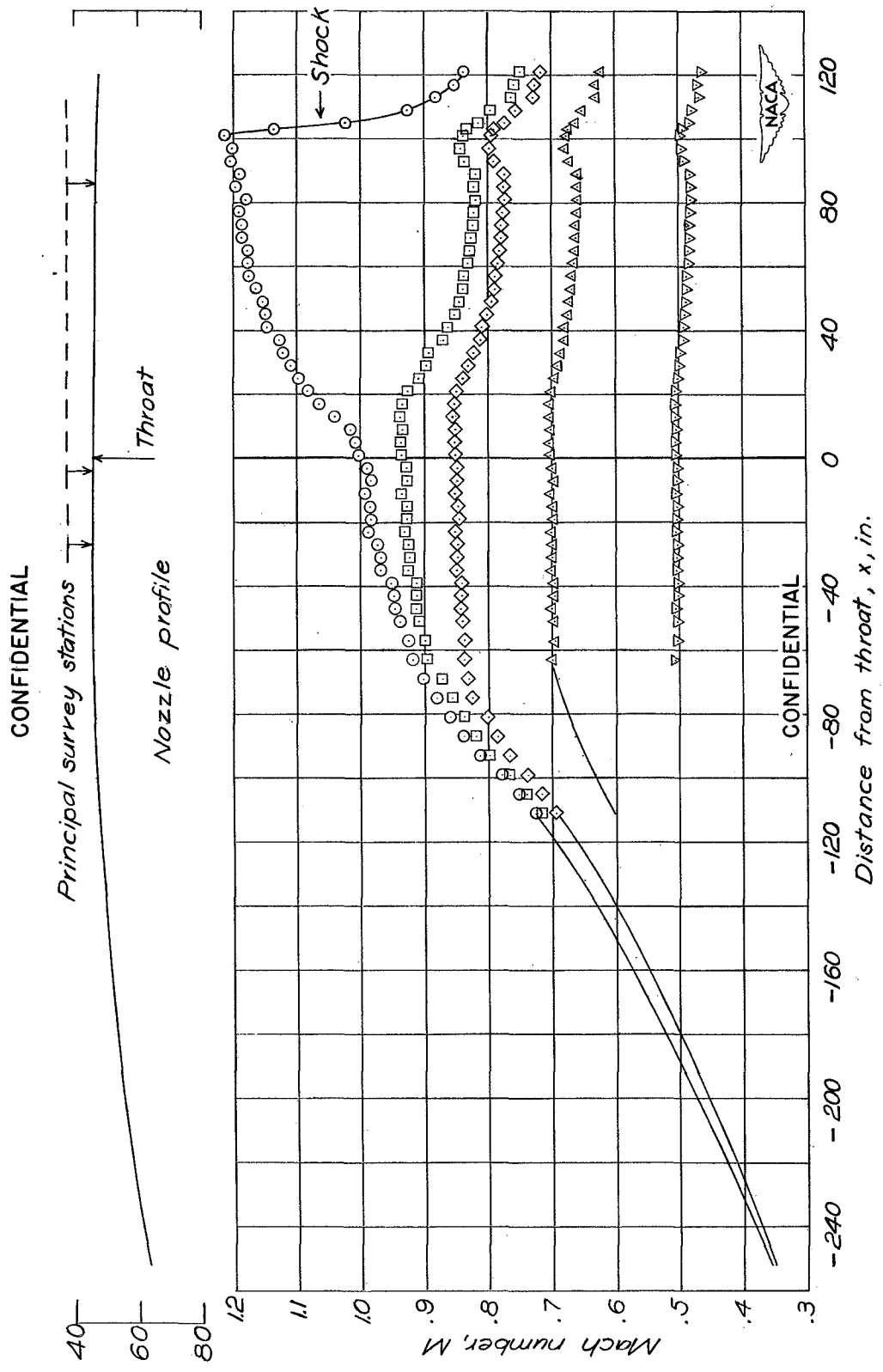

Figure 1.- Mach number distribution at nozzle wall. (Symbols represent runs at various speeds.)

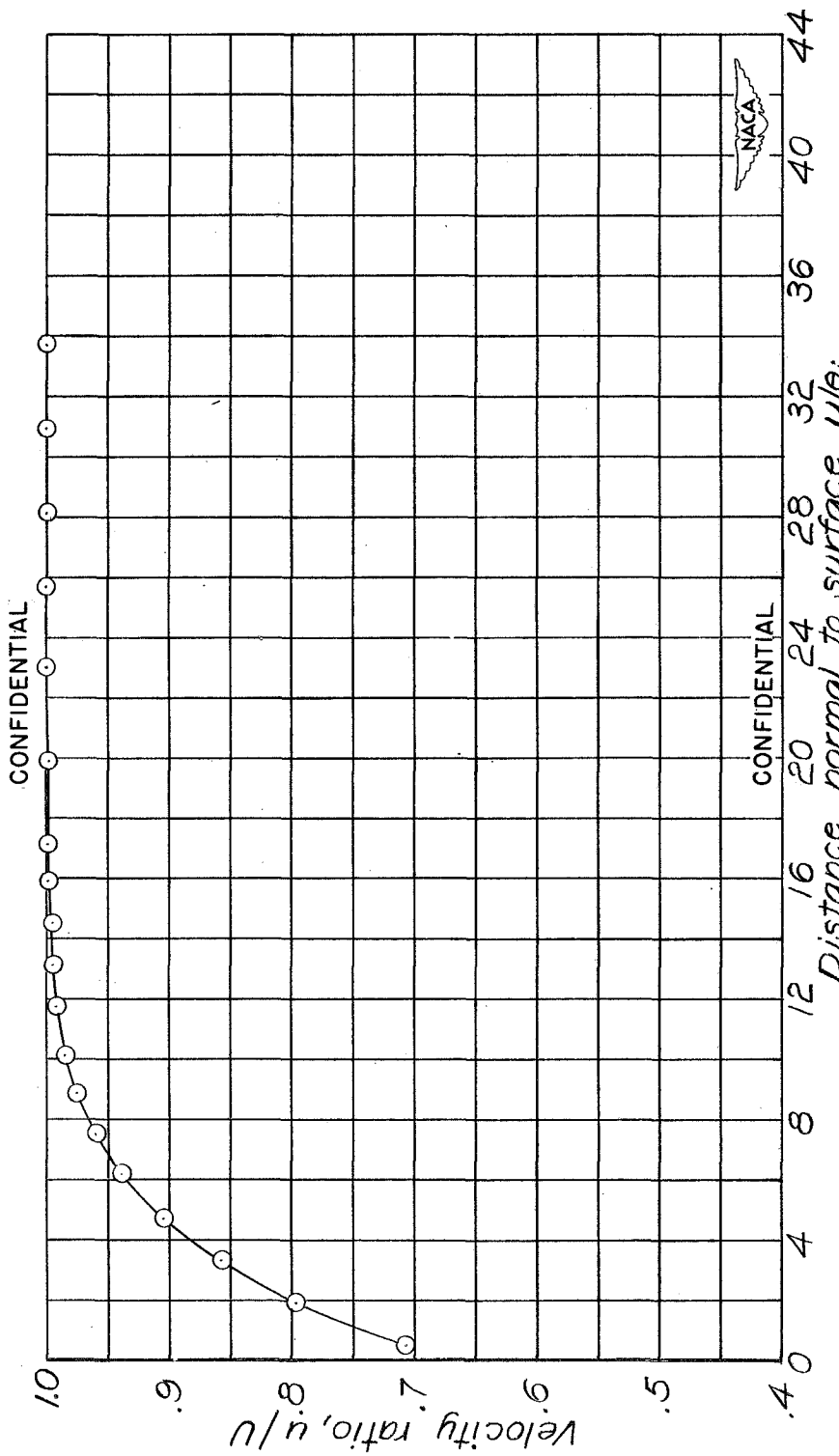

(a) M = 0.50; x = −27 inches; δ_c^* = 0.246 inch; δ_i^* = 0.228 inch; θ_c = 0.181 inch; θ_i = 0.183 inch; H_c = 1.355; H_i = 1.248; R_{θ_c} = 29,000.

Figure 2.- Typical boundary-layer velocity profiles. Approximate zero pressure gradient.

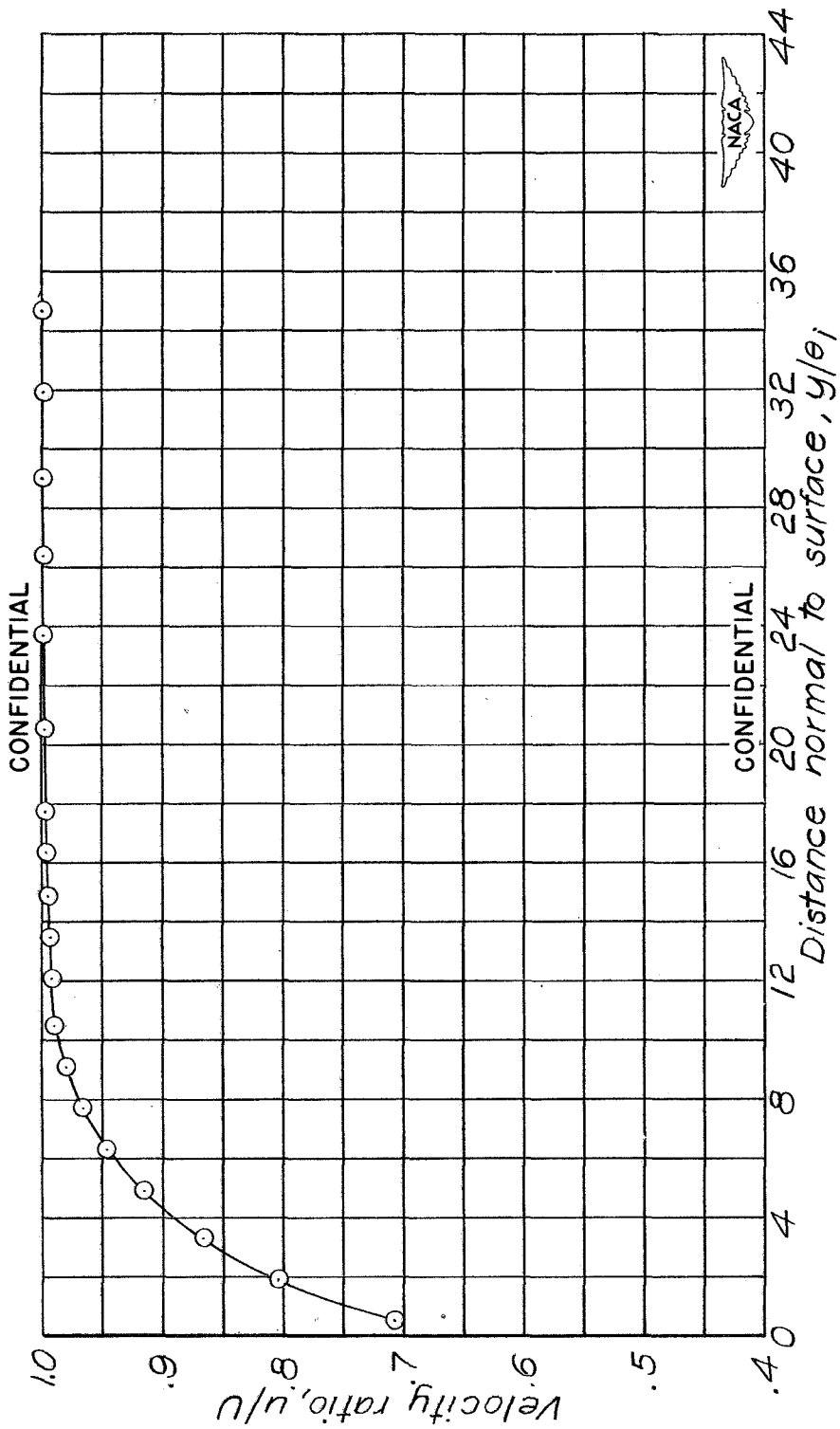

(b) M = 0.69; x = −27 inches; δ_c^* = 0.255 inch; δ_i^* = 0.223 inch; θ_c = 0.175 inch; θ_i = 0.178 inch; H_c = 1.463; H_i = 1.258; $R\theta_c$ = 33,400.

Figure 2.— Continued.

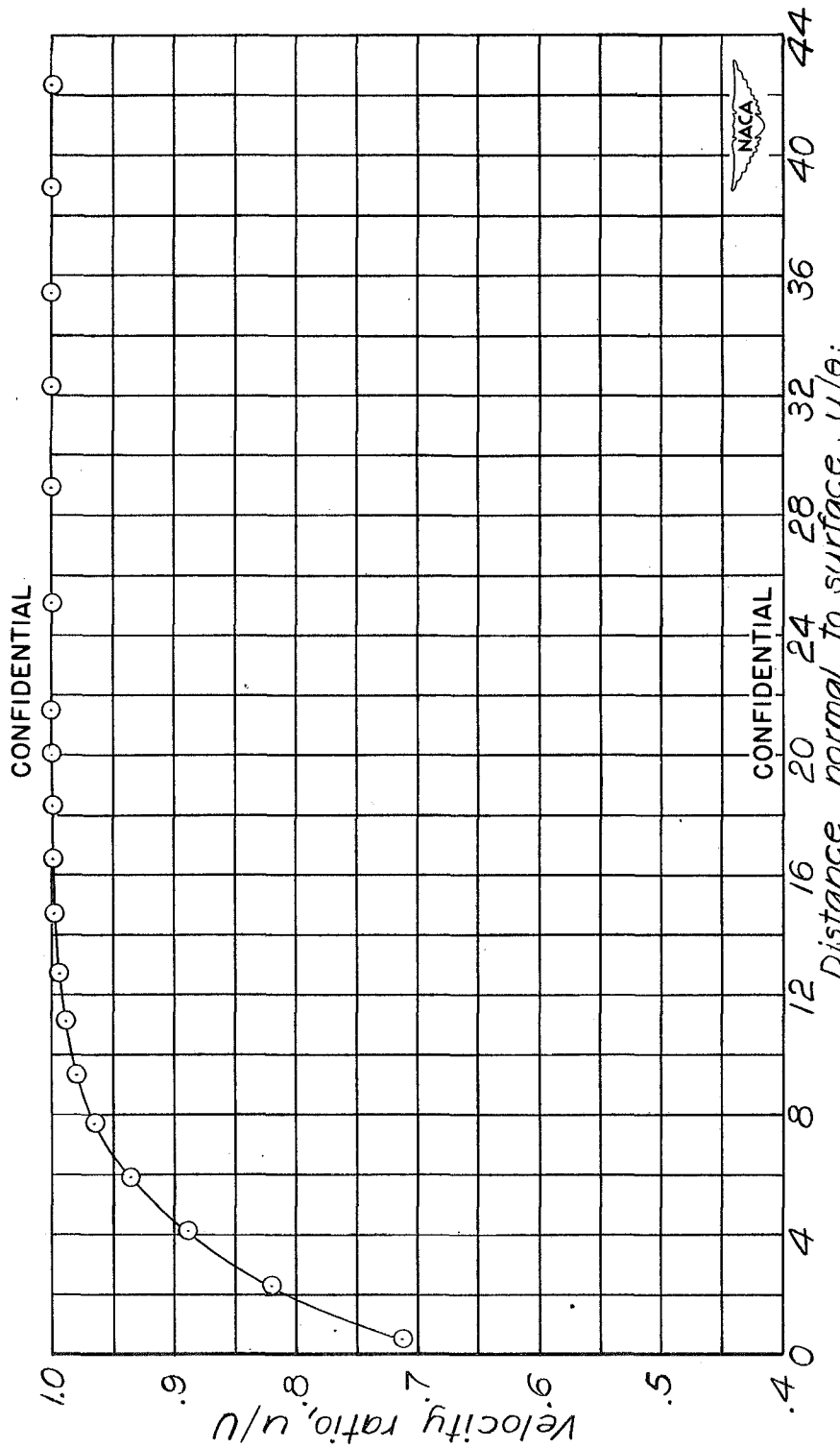

(c) M = 0.88; x = −27 inches; δ_c^* = 0.220 inch; δ_1^* = 0.186 inch; θ_c = 0.140 inch; θ_1 = 0.146 inch; H_c = 1.576; H_1 = 1.276; $R\theta_c$ = 28,700.

Figure 2.— Continued.

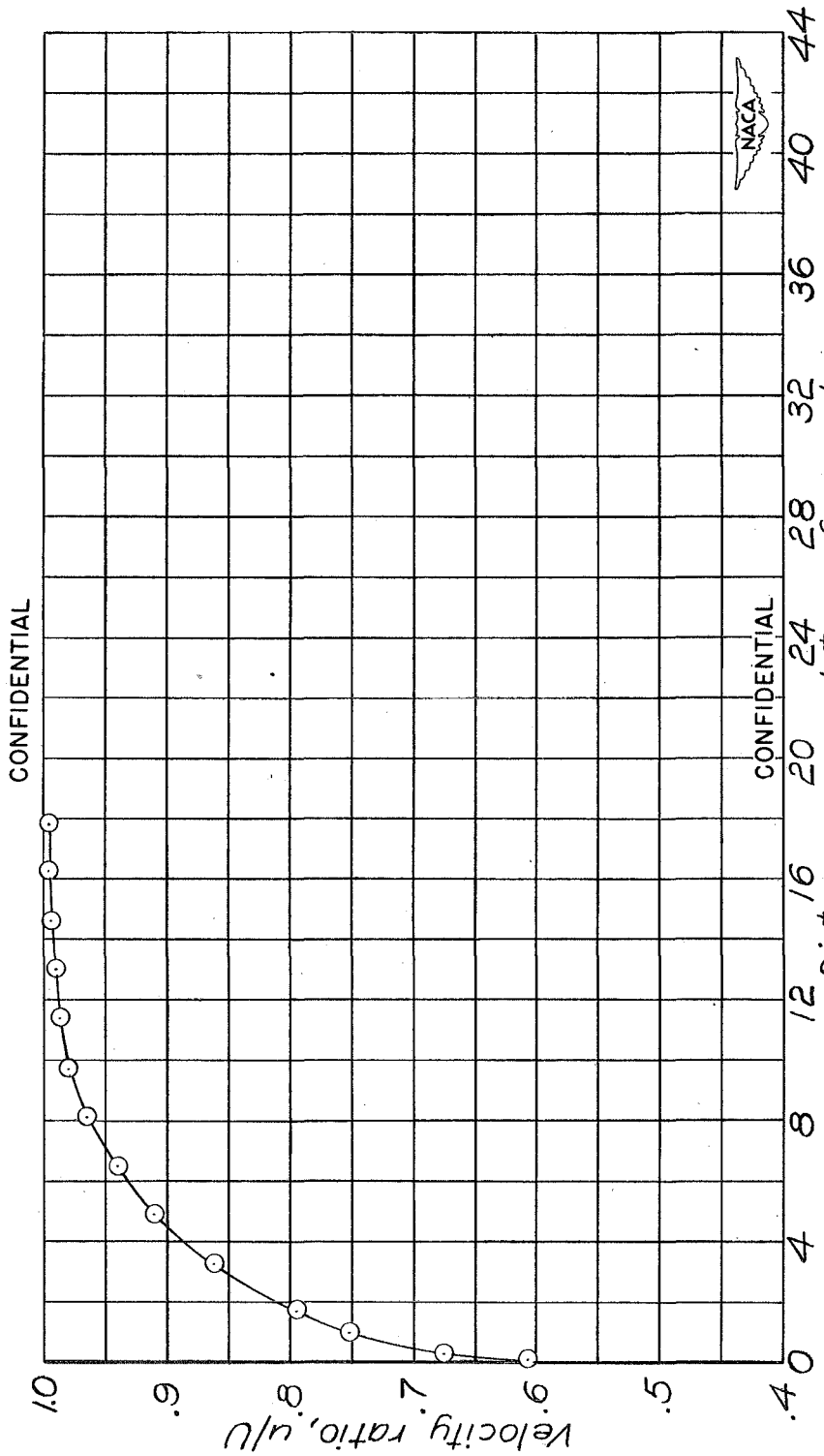

(d) $M = 0.97$; $x = 4$ inches; $\delta_c^* = 0.239$ inch; $\delta_i^* = 0.189$ inch; $\theta_c = 0.147$ inch; $\theta_i = 0.154$ inch; $H_c = 1.629$; $H_i = 1.225$; $R\theta_c = 27{,}900$.

Figure 2.- Continued.

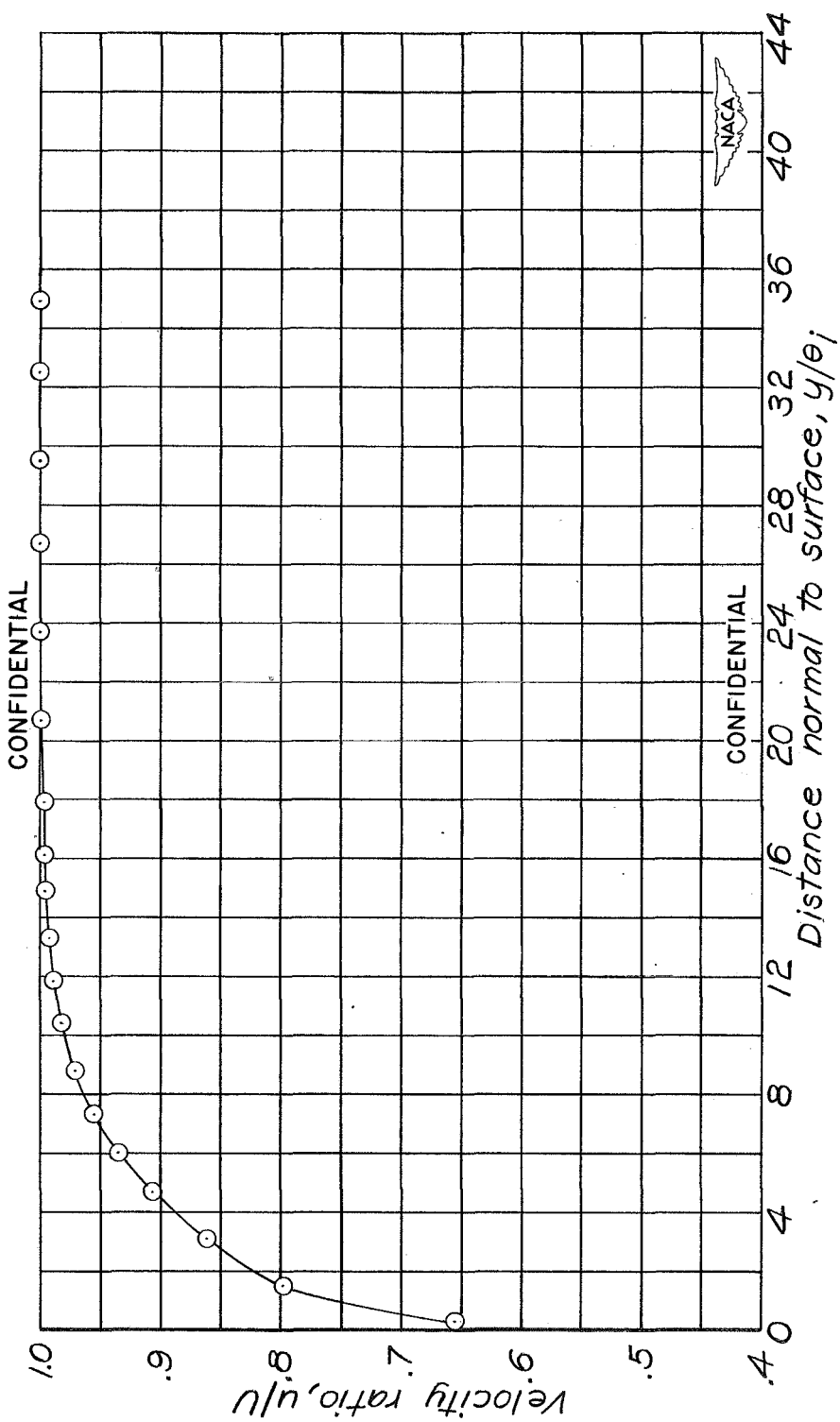

(e) M = 1.19; x = 86 inches; δ_c^* = 0.287 inch; δ_i^* = 0.204 inch; θ_c = 0.158 inch; θ_i = 0.172 inch; H_c = 1.819; H_i = 1.189; R_{θ_c} = 33,200.

Figure 2.- Concluded.

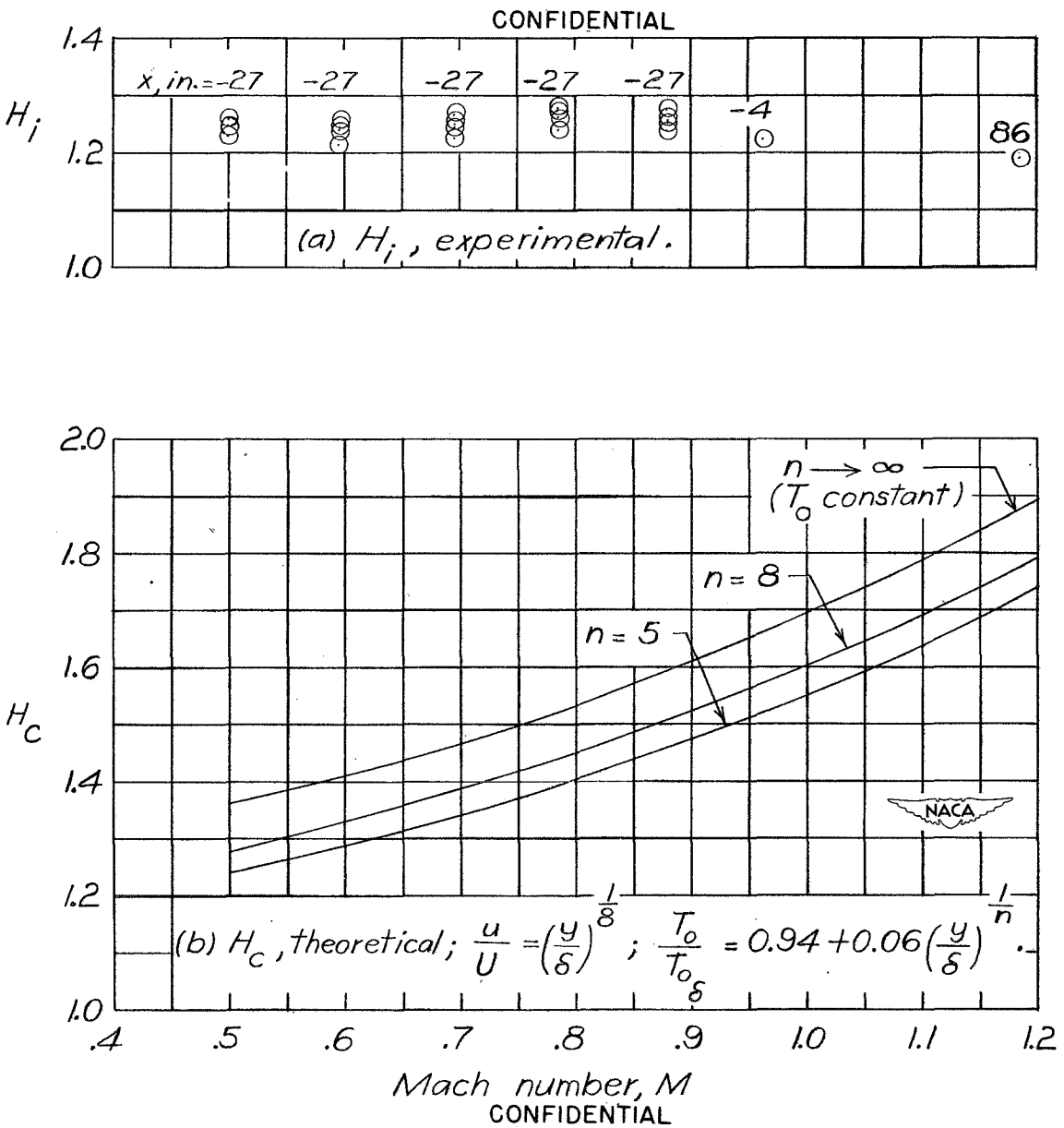

Figure 3.– Variation of the shape parameter H with Mach number.

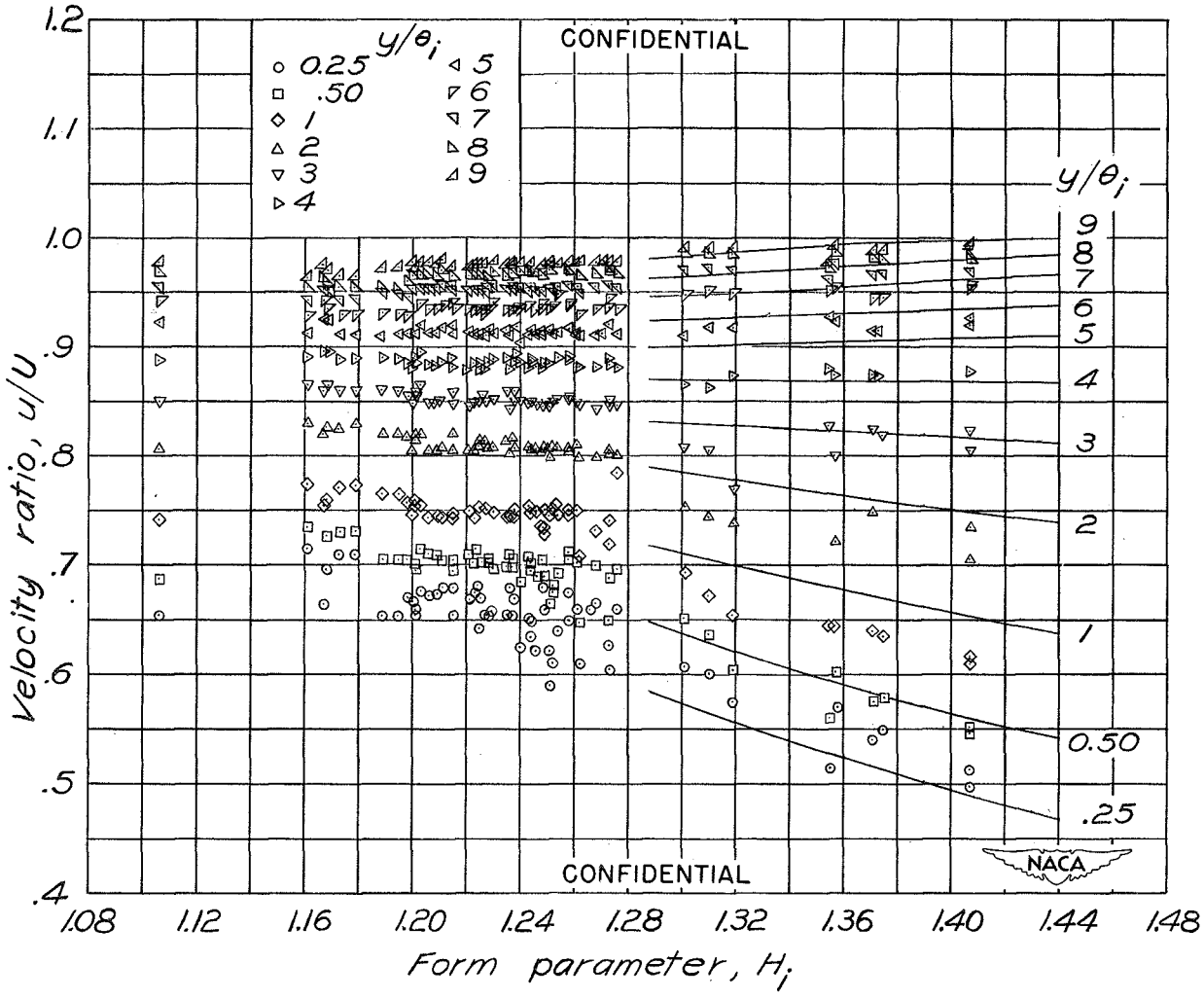

Figure 4.– Comparison of velocity profiles of present investigation with those of reference 2 with respect to incompressible form parameter H_i. (Symbols apply to present investigation and lines to that of reference 2.)

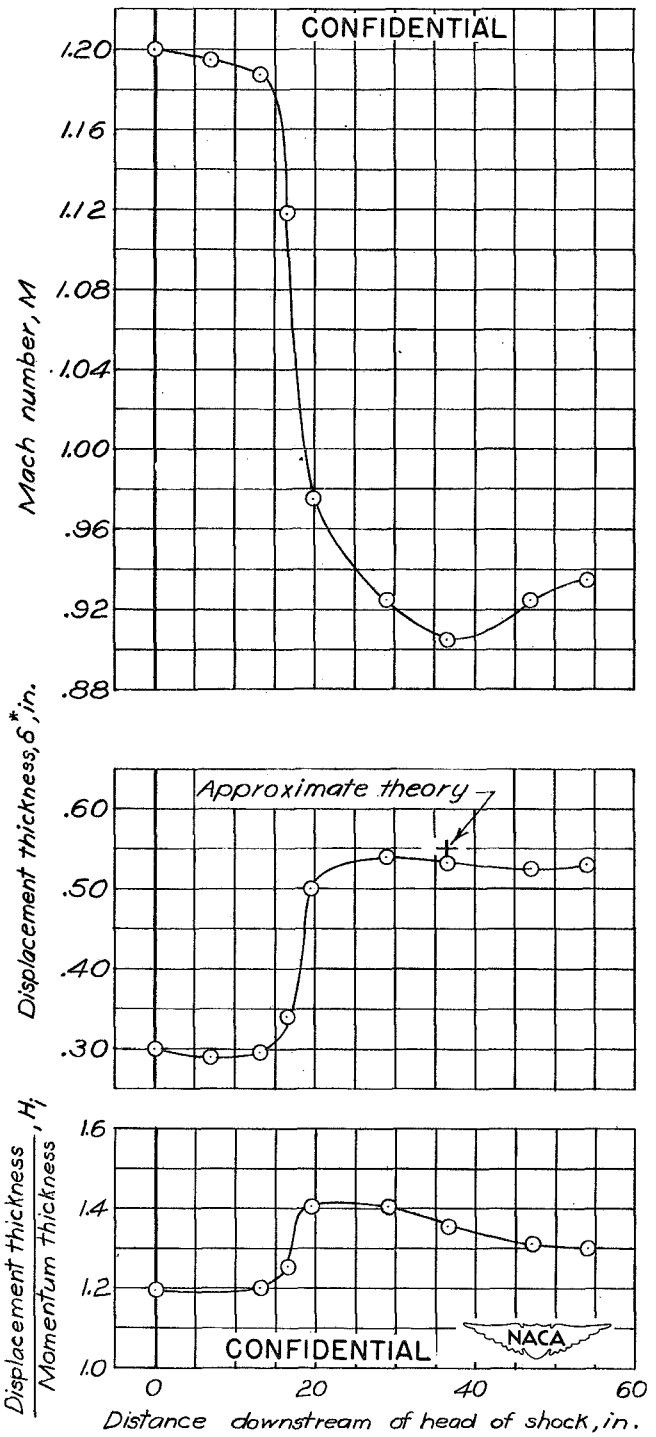

Figure 5.- Turbulent boundary-layer characteristics in the region of shock as measured on the wall of the Mach number 1.2 nozzle in the Langley 8-foot high-speed tunnel. Reynolds number per foot is 3.8×10^6.

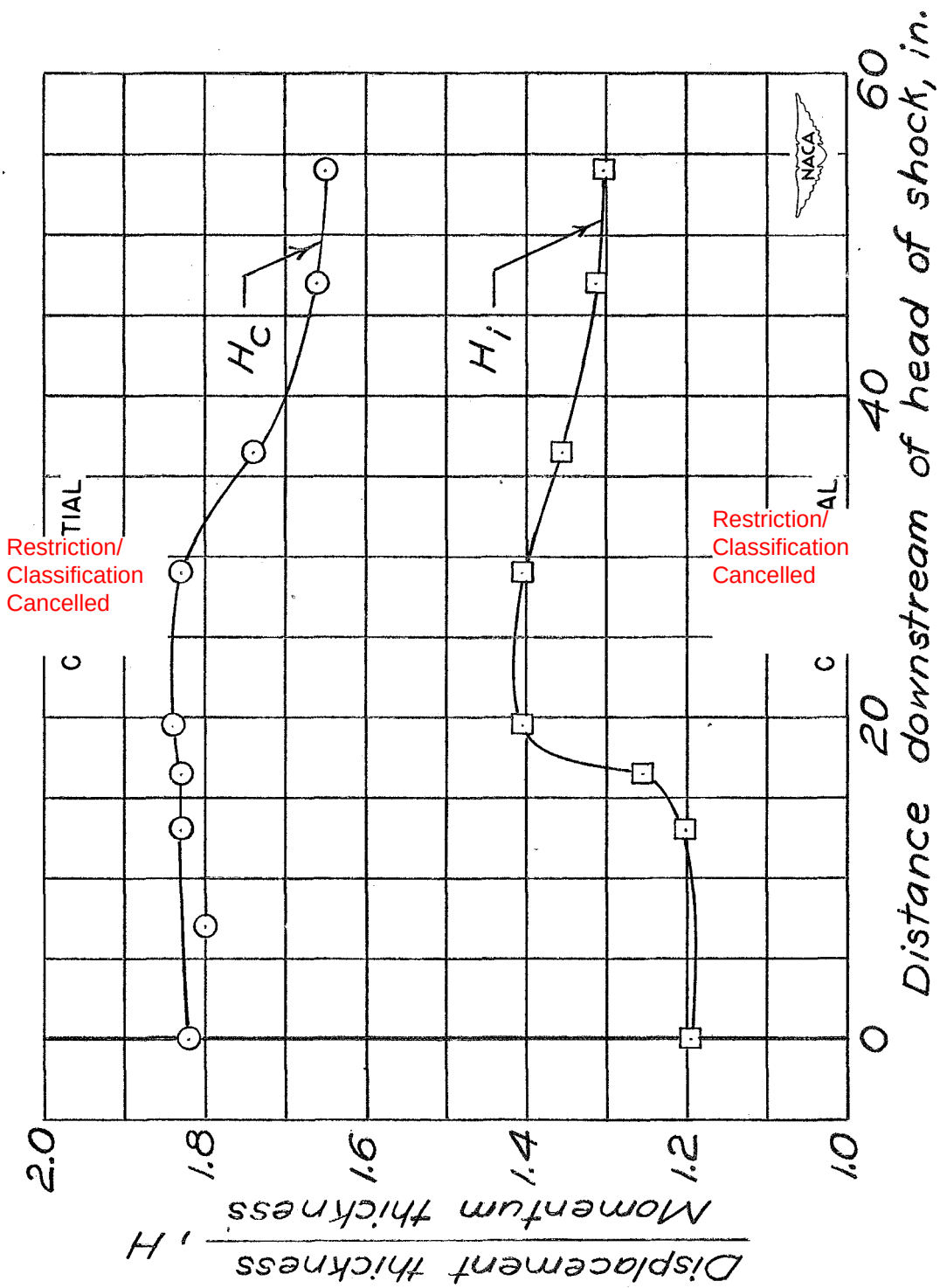

Figure 6.- Variation of form parameter under shock.